International Journal of Nanomedicine

Dovepress
Taylor & Francis Group

Open Access Full Text Article

ORIGINAL RESEARCH

Proteomic Landscape of Small Extracellular Vesicles Derived From Gastric Juice and Identified TFF2 as a Specific Biomarker

Ruiling Fan[1,*], Kaiwen Wu[2,*], Jingwei Yang[1,*], Binjun Zhu[3], Tao Jiang[3], Yu Liu[4], Bin Yuan[1], Lüye Liu[5], Yueshan Sun[5], Xiaobin Sun[6], Liu Liu[6], Wencai Luo[7], Chunyang Zhou[1], Yuanbiao Guo[5], Lei Liu[5]

[1]Institute of Materia Medica, School of Pharmacy, North Sichuan Medical College, Nanchong, Sichuan, 637007, People's Republic of China; [2]Department of Ultrasound, Shanghai Pulmonary Hospital, Tongji University School of Medicine, Shanghai, 200433, People's Republic of China; [3]North Sichuan Medical College, Nanchong, Sichuan, 637007, People's Republic of China; [4]Chinese Academy of Medical Science & Peking Union Medical College, Chengdu, Sichuan, 610052, People's Republic of China; [5]Medical Research Center, Affiliated Hospital of Southwest Jiaotong University, The Third People's Hospital of Chengdu, Chengdu, Sichuan, 610014, People's Republic of China; [6]Department of Gastroenterology, Affiliated Hospital of Southwest Jiaotong University, The Third People's Hospital of Chengdu, Chengdu, Sichuan, 610014, People's Republic of China; [7]Department of Gastroenterology, The People's Hospital of Guanghan, Deyang, Sichuan, 618300, People's Republic of China

*These authors contributed equally to this work

Correspondence: Lei Liu; Yuanbiao Guo, Medical Research Center, The Third People's Hospital of Chengdu, The Affiliated Hospital of Southwest Jiaotong University, 82# Qinglong Street, Chengdu, Sichuan, 610014, People's Republic of China, Email liulei@swjtu.edu.cn; guo.ybiao@yahoo.com

Introduction: Small extracellular vesicles (sEVs) derived from gastric juice (GJ) have emerged as potential biomarkers for gastric disease. However, methods for isolating sEVs from GJ (gsEVs) remain underexplored.

Methods: This study employed four methods for isolating gsEVs: ultracentrifugation (UC), PEG6000 precipitation combined with UC (PEG-UC), UC combined with size exclusion chromatography (UC-SEC), and ultrafiltration combined with SEC (UF-SEC). The yield and purity of gsEVs isolated by each method were evaluated, and the proteomic profile of gsEVs was examined through label-free quantitative proteomics. Additionally, a series of validation experiments were conducted to identify specific biomarkers for gsEVs.

Results: The results revealed that gsEVs isolated using the UC method exhibited the highest purity and the largest number of identified proteins compared to the other methods. Notably, the gastric tissue-specific peptide trefoil factor 2 (TFF2) was highly expressed in gsEVs isolated by all methods, suggesting that TFF2 may serve as a specific biomarker for gsEVs. Validation experiments showed that TFF2 was exclusively present in gsEVs and not in the GJ supernatant after UC. Furthermore, TFF2 was selectively expressed in gsEVs, but not in sEVs derived from other biofluids such as intestinal juice and plasma. The efficiency of TFF2 as a gsEVs biomarker was higher than the commonly used biomarker CD9, CD81, and Syntenin-1. Multi-omics analysis indicated that the functions of gsEVs carrying TFF2 were primarily associated with inflammation and cancer.

Conclusion: The UC method is suitable for isolating gsEVs, particularly for mass spectrometry-based proteomic analysis. The small peptide TFF2 may serve as a potential specific biomarker for gsEVs. This study offers new insights for research on sEVs in gastric diseases.

Keywords: gastric juice, small extracellular vesicles, proteomic, TFF2, biomarker

Introduction

Gastric juice (GJ) is a digestive secretion produced in the stomach, continuously generated at a rate of approximately 30 mL per hour. This production can double in response to various triggers, leading to a total output of 1.5–3.5 L of GJ per day.[1] The primary characteristic of GJ is its high concentration of H+, which is 3 million times greater than in blood and tissue.[2] Gastric hydrochloric acid (HCl) is produced by specialized parietal cells in the stomach. GJ also contains lipase and pepsin. The main functions of GJ are to digest food proteins and inactivate potential pathogenic microorganisms, thereby preventing intestinal infections.[3] In recent years, the role of GJ in diagnosing gastric diseases has garnered

Received: 22 January 2025
Accepted: 26 May 2025
Published: 29 May 2025

increasing attention. GJ analysis may be useful for many clinical purposes, including detecting H. pylori infection,[4] atrophic gastritis,[5] intestinal metaplasia,[6] and gastric cancer.[7]

Small extracellular vesicles (sEVs) are particles released from cells, consisting of a lipid bilayer with a diameter of < 200 nm.[8] Comprising proteins, nucleic acids, and metabolites, sEVs play a key role in mediating intracellular and intercellular communication, actively contributing to various physiological and pathological processes.[9] sEVs are found in most biofluids, such as blood,[10] urine,[11] saliva,[12] cerebrospinal fluid,[13] pleural effusion,[14] ascites,[15] amniotic fluid,[16] and semen.[17] Recently, gsEVs have also been studied. While blood is the primary source of sEVs for disease biomarker detection, the proportion of sEVs originating from pathological tissues in the blood is exceedingly low. In contrast, GJ, as a local biofluid, is expected to be enriched with gastric diseases-associated sEVs. Currently, gsEVs are primarily studied for their role in diagnosing gastric cancer (GC). Helicobacter pylori (H. pylori)-derived sEVs are elevated in the GJ of individuals with gastric adenocarcinoma and promote inflammation by interacting directly with gastric epithelial cells.[18] Methylation analysis of BARHL2 using exosomal DNA from GJ could serve as a potential tool for early GC diagnosis, independent of H. pylori infection.[19] Additionally, gsEVs also play a role in functional dyspepsia (FD). Exosomal hsa-miR-933 in GJ may be a potential biomarker for FD.[20] However, the function of gsEVs remains largely unexplored.

While sEVs have garnered significant interest as potential biomarkers, their application in basic research and clinical settings is restricted by the labor-intensive, inefficient, and time-consuming nature of their isolation processes.[21] The yield and purity of sEVs are significantly affected by their source and the processing methods employed.[22] For example, blood contains a large number of lipoprotein particles,[10] urine contains abundant protein such as Tamm-Horsfall Protein,[23] and bronchoalveolar lavage fluid contains surfactants,[24] all of which can be isolated alongside sEVs. Therefore, distinct approaches must be employed to effectively isolate sEVs from various biofluids. Currently, there are few studies on the isolation methods for GJ-derived sEVs. A primary challenge in isolating sEVs is removing nanoscale contaminants.[25] UC is the most widely employed technique for isolating sEVs. In addition to UC, SEC has been extensively used for size-based particle separation.[26] Other isolation techniques, such as polyethylene glycol (PEG) precipitation, widely used in clinical samples for its convenience, and ultrafiltration (UF), which is cost-effective and fast, are also applied. In this study, these methods were employed either individually or in combination to enhance the isolation efficiency of gsEVs.

sEV markers are important indicators for sEVs separation and identification. Currently, the tetraspanins CD9, CD63, and CD81 are the most frequently used biomarkers for sEVs. However, these markers exhibit heterogeneity in their ability to identify sEVs from various cell types, indicating that their use as biomarkers for sEVs derived from different cell origins may be limited.[27] Additionally, sEVs from different tissues and biofluids have specific biomarkers. Ldb3 has been proposed as a potential marker for cardiac sEVs, as it is predominantly detected in the neonatal rat heart relative to other tissues and shows specific expression in cardiomyocytes compared to cardiac fibroblasts.[28] PODXL, OCT4, Dnmt3a, and LIN28A have been identified as distinctive markers for sEVs derived from pluripotent stem cells (PSC-sEVs), selectively enriched in PSC-derived sEVs while being absent or minimally present in non-PSC-derived sEVs.[29] Therefore, we aim to identify specific biomarkers for gsEVs. In this study, proteomic analysis showed that TFF2 was high expressed in gsEVs isolated by all methods. TFF2 was found exclusively in gsEVs and not in the GJ supernatant after UC. Additionally, TFF2 was specifically expressed in gsEVs but not in sEVs derived from intestinal juice and plasma. These results suggest that TFF2 may be a potential specific biomarker for gsEVs. This study could provide novel insights for research on sEVs in gastric diseases.

Methods

Samples Collection

GJ samples were collected from four healthy individuals (2 males and 2 females) during gastroscopy at the Third People's Hospital of Chengdu. All participants fasted for 12 hours before the examination. Intestinal juice samples were obtained from four healthy individuals during colonoscopy. Fasting venous blood samples were collected using EDTA anticoagulant tubes and subjected to a two-step centrifugation process at 2500 ×g for 15 minutes at room temperature to remove platelets and blood cells. GJ samples from the four individuals were used to compare various isolation methods,

while GJ, intestinal juice, and blood samples from the four individuals were used to validate the specificity of gsEVs biomarkers. The study was approved by the Ethics Committee of the Third People's Hospital of Chengdu (2024-S-212), and written informed consent was obtained from all participants.

Isolation of sEVs

For gsEV isolation, 80 mL of GJ derived from four individuals was mixed and diluted 1:1 with PBS. The GJ was subjected to a series of centrifugations to remove contaminant particles: spun at 300 ×g for 10 minutes to eliminate food residues and cells, 2000 ×g for 30 minutes to remove cell debris, and 10,000 ×g for 60 minutes to eliminate microvesicles. The supernatant was passed through 0.22 μm membranes and aliquoted for further study. The isolation of sEVs from intestinal fluid and plasma followed a similar pre-treatment method as that of GJ.

UC

For the UC method, the supernatant was subjected to UC at 110,000 ×g for 70 minutes at 4°C using a Beckman L-100XP ultracentrifuge (CA, USA). The resulting pellet was resuspended in PBS and underwent a second UC under the same conditions. The pellet was then reconstituted in PBS for sEV characterization and LC-MS/MS analysis.

PEG6000 Precipitation (PEG)

For the PEG method, a 50% (w/v) PEG6000 stock solution (BioFroxx, Munich, Germany) was prepared using ultrasonic mixing and passed through a 0.22 μm membrane. The pre-treatment GJ samples were combined with the PEG6000 stock to achieve a final PEG concentration of 10%, along with 75 mm NaCl by adding 3.75 M NaCl stock. The mixture was gently inverted to ensure uniform distribution and maintained at 4 °C for 14 hours. gsEVs were separated by centrifugation at 4500 × g for 30 minutes at 4 °C. The supernatant was discarded, and the precipitate was rinsed with 11 mL of PBS to remove residual PEG and contaminants. The sample was then centrifuged at 110,000 ×g for 70 minutes at 4°C. The resulting pellet was resuspended in 500 μL of PBS and stored at −80 °C for further analysis.

SEC

For the SEC method, a qEV original 35 nm size exclusion column (IZON, Christchurch, NZ) was used according to the manufacturer's instructions. The columns were equilibrated with 20 mL of PBS prior to use. Next, 500 μL of pre-treated GJ samples were applied to the column and eluted with PBS. The eluate was divided into 13 fractions of 1 mL each and stored at −80°C for further analysis.

UF

For the UF method, pre-treated GJ samples were subjected to UF using a 100-kDa molecular weight cutoff filter (Millipore, MA, US), retaining particles greater than 100 kDa, including sEVs, while removing smaller molecules such as albumin. This process concentrated 15–20 mL of GJ to a final volume of 300–500 μL. For further purification, the retained fraction was processed by SEC. The resulting pellet was re-dissolved in 500 μL of PBS for further examination.

Characterization of sEVs

Nanoparticle Tracking Analysis (NTA)

The size and concentration of sEV particles were measured using NTA with a ZetaView instrument (Particle Metrix, Meerbusch, Germany). The samples were diluted to 50–200 particles per frame using filtered PBS. The instrument analysis parameters were set as follows: sensitivity at 70, shutter at 70, minimum brightness at 20, maximum area at 1000, minimum area at 5, and laser wavelength set to 488 nm. Each measurement was performed at 11 positions, and the data were analyzed using ZetaView software (version 8.05.11).

Bicinchoninic Acid (BCA) Assay

The protein concentration of sEVs isolated by various methods were determined using the Pierce BCA Protein Assay Kit (Thermo Scientific, IL, USA) according to the manufacturer's instructions.

Transmission Electron Microscopy (TEM)

The morphology of sEVs was examined using TEM (JEOL, JEM-1400, Tokyo, Japan). Briefly, freshly isolated sEVs were applied to a copper grid and kept at room temperature for five minutes. The grid was then treated with 2% (v/v) uranyl acetate and observed immediately after staining.

Western Blotting (WB)

Protein samples were loaded into 12% TGX Stain-Free gels (Bio-Rad, CA, USA) in equal amounts or volumes. Prior to transferring proteins onto polyvinylidene fluoride (PVDF) membranes, the gels were exposed to UV light to detect total protein loading using the Stain-Free technique and a Bio-Rad ChemiDoc MP imaging system. The membranes were incubated in a blocking solution of TBS supplemented with 0.1% Tween and 5% milk for 2 hours at ambient temperature. Subsequently, the membranes were incubated overnight at 4°C with primary antibodies diluted 1:1000 in blocking buffer. For CD63, human samples were probed with anti-CD63 (13,681-1-AP, Proteintech, Wuhan, China), and murine samples with anti-CD63 (ab217345, Abcam, Cambridge, UK). For CD9, human samples were incubated with anti-CD9 (20,597-1-AP, Proteintech), and mouse samples with anti-CD9 (ab307085, Abcam). For TFF2, murine samples were treated with anti-TFF2 (13,681-1-AP, Proteintech), while human samples were incubated with anti-TFF2 (ab267474, Abcam). For CD81 (27,855-1-AP), Alix (12422-1-AP), TSG101 (28,283-1-AP), and Calnexin (66903-1-Ig), the same antibody was used for both species. All antibodies, unless otherwise noted, were obtained from Proteintech (Wuhan, China). The next day, the membranes were rinsed in TBST and incubated for 1.5 hours with HRP-conjugated secondary antibodies (Cell Signaling Technology, MA, US). After incubation, an additional wash with TBST was performed. Protein bands were visualized using enhanced chemiluminescence (ECL) reagents (Millipore, MA, US) according to the manufacturer's guidelines. The resulting immunoblots were imaged and analyzed using the ChemiDoc MP Imaging System. For WB quantification, band intensities were measured using ImageJ software (NIH, USA). To account for loading variations, Stain-Free total protein normalization was used as the loading control, instead of relying on housekeeping proteins, due to the absence of established internal markers for EVs. Densitometric values were normalized to total lane protein intensity.

Nano-Flow Cytometry (NanoFCM) Analysis

Purified gsEVs were analyzed using a flow nanoparticle analyzer (NanoFCM Inc., Xiamen, China) with 488 nm and 640 nm lasers. Fluorescent signal calibration was achieved using 250 nm silica nanospheres conjugated with fluorescent dyes, under 20 mW laser power, 0.2% side scatter attenuation, and a sampling pressure of 1 kPa. For surface protein staining, gsEVs isolated by the four methods were used, and the concentration and size were determined using unstained samples. Ten μL gsEV samples (2–6 × 10^{10} particles/mL) from each method were incubated with 1 μL of FITC-labeled CD63, CD9, CD81, or IgG antibodies (BioLegend, CA, US), diluted 10-fold in PBS at 37°C in the dark for 30 minutes. The stained samples were then diluted 100-fold to ensure an event rate of 4000–8000 events per minute. For both gsEVs and blank controls, the instrument settings included 10 mW laser power, a 488 nm laser, 10% side scatter attenuation, 1 kPa sampling pressure, and a 1-minute acquisition time. FITC signals were detected using a 525/40 filter, and data analysis was performed using NF Profession 1.17 and FlowJo v10.8.1.

Label-Free Quantitative Proteomics

Protein Extraction and Digestion

The specimens were sonicated for three minutes on ice using a high-power ultrasonic processor (Scientz, Ningbo, China). The samples were then centrifuged at 12000 g for 10 minutes at 4 °C. The supernatant was quantified using a BCA assay kit (Beyotime, Shanghai, China). A 30 μg protein sample was enzymatically hydrolyzed. The digestion process began with reduction using 5 mm dithiothreitol at 56°C for 30 minutes, followed by alkylation with 11 mm iodoacetamide for 15 minutes at room temperature in the dark. The protein sample was diluted with 200 mm TEAB to reduce the urea concentration to below 2M. Trypsin was then added at a 1:50 trypsin-to-protein mass ratio for overnight digestion, followed by a secondary digestion with a 1:100 trypsin-to-protein mass ratio for four hours. The resulting peptides were purified using a Strata X SPE column, and peptide quantification was performed post-digestion.

Lc-Ms/Ms

Peptides were dissolved in Solution A (0.1% formic acid and 2% acetonitrile in water) and loaded onto a reversed-phase column (25 cm long, 75/100 mm in diameter). To separate the peptides, label-free proteomics was used with a gradient of solvent B (0.1% formic acid in acetonitrile). The gradient started at 6%, gradually increasing to 24% over 70 minutes, then from 24% to 35% over 14 minutes, followed by an increase to 80% for 3 minutes, and finally maintaining 80% for the remaining 3 minutes. All steps were performed at a constant flow rate of 450 nL/min on a nanoElute UHPLC system (Bruker Daltonics, Karlsruhe, Germany). Analysis was conducted using a capillary ion source on the timsTOF Pro mass spectrometer (Bruker Daltonics, Karlsruhe, Germany), with an electrospray voltage of 1.60 kV. Precursor ions and their fragments were detected with a TOF detector, covering a mass range of 100 to 1700 m/z for the MS/MS scan. The timsTOF Pro was operated in parallel accumulation serial fragmentation (PASEF) mode, selecting precursor ions with charge states from 0 to 5 for fragmentation. Ten PASEF-MS/MS scans were obtained per cycle, with dynamic exclusion set to 30 seconds to minimize repetitive ion analysis.

Data Analysis

MaxQuant (v.1.6.15.0) was used for peptide detection and measurement of all DDA data. MS2 spectra were queried against the complete set of protein sequences (Homo_sapiens_9606_SP_20210721.fasta) obtained from UniProt. Trypsin/P was specified as the proteolytic enzyme, with a limit of 2 missed cleavage sites. The precursor ion tolerance was set at 20 ppm, and the fragment mass tolerance was set to 20 ppm. The minimum peptide length was set to seven amino acids. For proteome analyses, carbamidomethylation of cysteine was set as a constant modification, while methionine oxidation and N-terminal protein acetylation were set as dynamic modifications. The false positive rate (FDR) was assessed using an anti-library. The impact of contaminating proteins on identification outcomes was mitigated by a common contamination library. The FDR for protein and PSM identification was controlled at 1%. The database search results were further refined to ensure high-quality analytical outcomes. The FDR accuracy was maintained at 1% for spectra, peptide fragments, and proteins. Protein qualitative analysis required at least one unique peptide, while quantitative analysis required a minimum of two unique peptides.

Bioinformatics Analysis

Venn analysis of proteins was performed on BioVenn (http://www.biovenn.nl/index.php). Gene Ontology (GO) annotation of cellular compartment was performed using FunRich (Version 3.1.3). A heatmap for comparing and visualizing protein expression levels was also generated by FunRich (Version 3.1.3). Gene expression profiling in human tissues was analyzed and visualized on GEPIA (http://gepia.cancer-pku.cn/index.html).

Cell Experiment

Cell Culture

The human gastric mucosal cell line GES-1 were obtained from the Type Culture Collection of the Chinese Academy of Sciences (Shanghai, China) and maintained in RPMI 1640 medium containing 10% FBS, 100 U/mL penicillin, and 100 μg/mL streptomycin. All cell lines were incubated at 37 °C in a humidified incubator with 5% CO_2.

Lentivirus Infection

Lentiviruses encoding overexpressed TFF2 (TFF2) and control vector (NC) were packaged by GenePharma Company (Shanghai, China). The nucleotide encoding sequences were based on the mRNA of Homo sapiens TFF2 (>NM_005423.5:38–427). Cells in the logarithmic growth phase were harvested and seeded into a 24-well plate at a density of 5×10^4 cells per well. After cell attachment, the cells were transduced with lentivirus and, two days later, selected using 2 μg/mL puromycin. TFF2 expression in each cell clone was detected by WB, and the most efficiently overexpressed cells were used in subsequent studies.

Isolation of sEVs From Cell Supernatant

To collect secreted sEVs from cells, the cells were grown to 80–90% confluence and then cultured in sEVs-depleted medium. After 24 hours, the sEVs-depleted medium was collected. The medium underwent a series of

centrifugations to remove cell debris and microvesicles: 300 ×g for 10 minutes, 2000 ×g for 30 minutes,10000×g for 60 minutes, and then UC at 100000 g for 70 minutes. After discarding the supernatant, the pellets were washed with PBS and centrifuged at 100,000 ×g for 70 minutes. The sEVs were resuspended in PBS and used for subsequent experiments.

Flow Cytometry of Bead-Bound sEVs

The sEVs derived from GJ or cell lines were suspended in PBS and incubated with aldehyde/sulfate beads (Invitrogen, CA, US) at a 5 μg EV to 1 μL bead ratio. After a 15-minute incubation at ambient temperature with constant rotation, the samples were diluted to a final volume of 300 μL in PBS and then incubated for 12 hours at 4°C. On the following day, 100 mm glycine and 2% BSA in PBS were added to halt the reaction, and the mixture was rotated for an additional hour at room temperature. EV-bound beads were pelleted by centrifugation at 10,000×g for 3 minutes, after which the supernatant was discarded. Beads were washed twice with 200 μL of 2% BSA and centrifuged for 3 minutes at 10,000 ×g, with the resulting pellets used for subsequent staining procedures.

Surface sEV protein staining was performed by incubating EV-bound beads with conjugated antibodies (CD63, CD9, CD81, and IgG), followed by vortexing and gentle rotation at standard temperature for 1 hour. After incubation, the beads were washed twice in 200 μL of 2% BSA. Intraluminal proteins were stained after a fixation/permeabilization step using 100 μL of Fixation/Permeabilization reagent (eBioscienc, CA, US), followed by washing with 200 μL of 1x Permeabilization buffer (eBioscience, CA, US). The beads were then incubated with conjugated antibodies (TFF2 and IgG) on ice for 1 hour. All subsequent wash steps for intraluminal staining were carried out in 200 μL of Permeabilization buffer. Following surface staining, sEVs-bound beads were transferred into 500 μL of 2% BSA solution for resuspension, and following intraluminal staining, they were re-suspended in 500 μL of Permeabilization buffer. Flow cytometry was performed using a Beckman instrument.

Immunogold Labeling and Electron Microscopy

The freshly prepared gsEVs suspensions were dispersed in a solvent matching the composition of the original test solution. A 300-mesh carbon/formvar-coated grid was loaded with the suspension and allowed to adsorb for 5 minutes at room temperature. The grid was gently rinsed with the dispersant for 10 seconds to remove excess material, followed by sequential washes with PBS and glycine buffer. To minimize nonspecific interactions, the grids were blocked with 0.5–2% PBS-BSA for 30 minutes. For immunogold labeling, the grids were incubated with a primary antibody solution (anti-CD63, anti-Syntenin-1, or anti-TFF2; Proteintech, Wuhan, China) diluted 1:50 for 1 hour at room temperature or 37°C. Blank control grids were prepared by omitting the primary antibody. After incubation, the support films were washed thoroughly with PBS and incubated in a conjugated antibody solution with 30 nm gold nanoparticles (Solarbio, Beijing, China) for 1 hour at room temperature. Unbound reagents were removed by sequential rinses with PBS and distilled water. Electron staining was carried out by incubating the grids with 2% aqueous uranyl acetate for 15 minutes, followed by lead citrate for 1 minute. Finally, the grids were air-dried overnight at room temperature. High-resolution electron micrographs were acquired using a HITACHI transmission electron microscope for sample visualization and analysis.

Animal Experiments

In this research, 12 male C57BL/6 mice (8 weeks old, weighing 20–25g) were obtained from Charles River Company (Beijing, China) and maintained under controlled environmental conditions (25 ± 2°C, 12-hour light/dark cycle) with unrestricted access to a standard laboratory diet and water. All experimental procedures were approved by the Ethics Committee of Southwest Jiaotong University Approval (Agreement No. SWJTU-2103-026). Prior to sampling, the mice were subjected to an overnight fasting period. Following anesthesia, gastric and intestinal fluids were collected and processed via differential centrifugation. Blood samples were drawn from the retro-orbital sinus using capillary tubes, then centrifuged at 2500 ×g for 15 minutes to separate platelets and blood cells. sEVs were subsequently isolated from gastric fluid, intestinal fluid, and plasma by UC, followed by NTA, TEM, and WB.

Transcriptome Sequencing

Transcriptome sequencing commenced with quality-checked total RNA, followed by mRNA isolation using poly-T oligo beads, fragmentation, and cDNA synthesis. Size-selected libraries (370–420 bp) were amplified, assessed for quality, and sequenced on the Illumina NovaSeq 6000 to generate paired-end 150 bp reads. Reads were quality-filtered (Q20, Q30), aligned to the reference genome with Hisat2, and quantified in FPKM with featureCounts. Differential expression analysis was conducted with DESeq2 or edgeR, depending on replicate availability. Enrichment analyses (GO, KEGG) provided insights into expression dynamics across biological states, and protein-protein interactions were analyzed using STRING or Diamond.

Statistical Analysis

Statistical analyses were performed using GraphPad Prism 8, with all experiments repeated at least three times. Differences between two groups were assessed using Student's *t*-test, and a p-value of less than 0.05 was considered statistically significant.

Results

Impact of Isolation Methods on gsEV Yield and Purity

To identify the optimal method for gsEV isolation, four techniques were employed in this study: UC, PEG-UC, UC-SEC, and UF-SEC (Supplementary Figure 1). NTA revealed that all four methods resulted in gsEVs with particle sizes below 150 nm (Figure 1A). However, the yield and purity varied among the methods. The UC method yielded the highest particle concentration, approximately 1×10^{12} particles/mL, while the PEG-UC method produced the lowest concentration at around 5×10^{11} particles/mL. The UC-SEC and UF-SEC methods had particle concentrations of approximately 7×10^{11} particles/mL and 9×10^{11} particles/mL at fraction 4, respectively. Given that not all particles detected by NTA represent genuine sEVs, particle counts were normalized to the protein content, calculating the number of particles per microgram of protein. This analysis showed that fraction 4 from the UC-SEC and UF-SEC methods exhibited the highest particle concentrations, at approximately 1.5×10^{10} and 2×10^{10} particles/μg, respectively, while UC and PEG-UC methods yielded 5×10^{9} and 2.5×10^{9} particles/μg, respectively (Figure 1B). In the UC-SEC method, protein concentration peaked in fractions 9 to 11, whereas in the UF-SEC method, the peak was observed in fractions 7 to 13 (Supplementary Figure 2A), differing significantly from the particle count distribution. These results suggest that UC-SEC and UF-SEC effectively removed contaminating proteins. TEM revealed cup-shaped particles indicative of lipid bilayer structures, with gsEVs from all methods having an approximate diameter of 100 nm. While the gsEVs isolated by UC appeared relatively pure, those isolated by the other three methods were surrounded by non-sEV particles such as lipids and protein aggregates (Figure 1C), suggesting higher purity for the UC method.

Additionally, the presence of sEVs markers was confirmed through WB and NanoFCM. WB detected four sEVs markers (Alix, CD63, CD9, and TSG101) and a non-sEVs marker, Calnexin. All sEV markers were detected in the UC and PEG-UC groups. Consistent with the particle counts per microgram of protein, the highest expression of sEV markers was observed in fraction 4 of the UC-SEC and UF-SEC methods. Notably, the non-sEV marker Calnexin was undetected across all methods (Figure 1D). As total protein quantification was used for normalization, the protein content in UF-SEC peaked in fractions 8 to 12 (Supplementary Figure 2B), yet the highest sEV marker expression occurred in fraction 4, confirming the effective removal of contaminants. NanoFCM analysis showed that CD9, CD81, and CD63 were present in all samples, though their expression levels varied. CD63-positive particles were most abundant, followed by CD9, while CD81-positive particles were barely detectable The lowest detection rates for CD63 and CD9 were found in the UF-SEC method (Figure 1E). These findings demonstrate that while all four methods effectively isolate gsEVs, their yield and purity differ significantly.

Proteomic Profiling of gsEVs Isolated by Different Methods

To assess the proteomic profiles of gsEVs, label-free quantitative proteomic analysis (LC-MS/MS) was performed. Since the PEG-UC method yielded the lowest amount of gsEVs, samples from the other three methods were analyzed. The

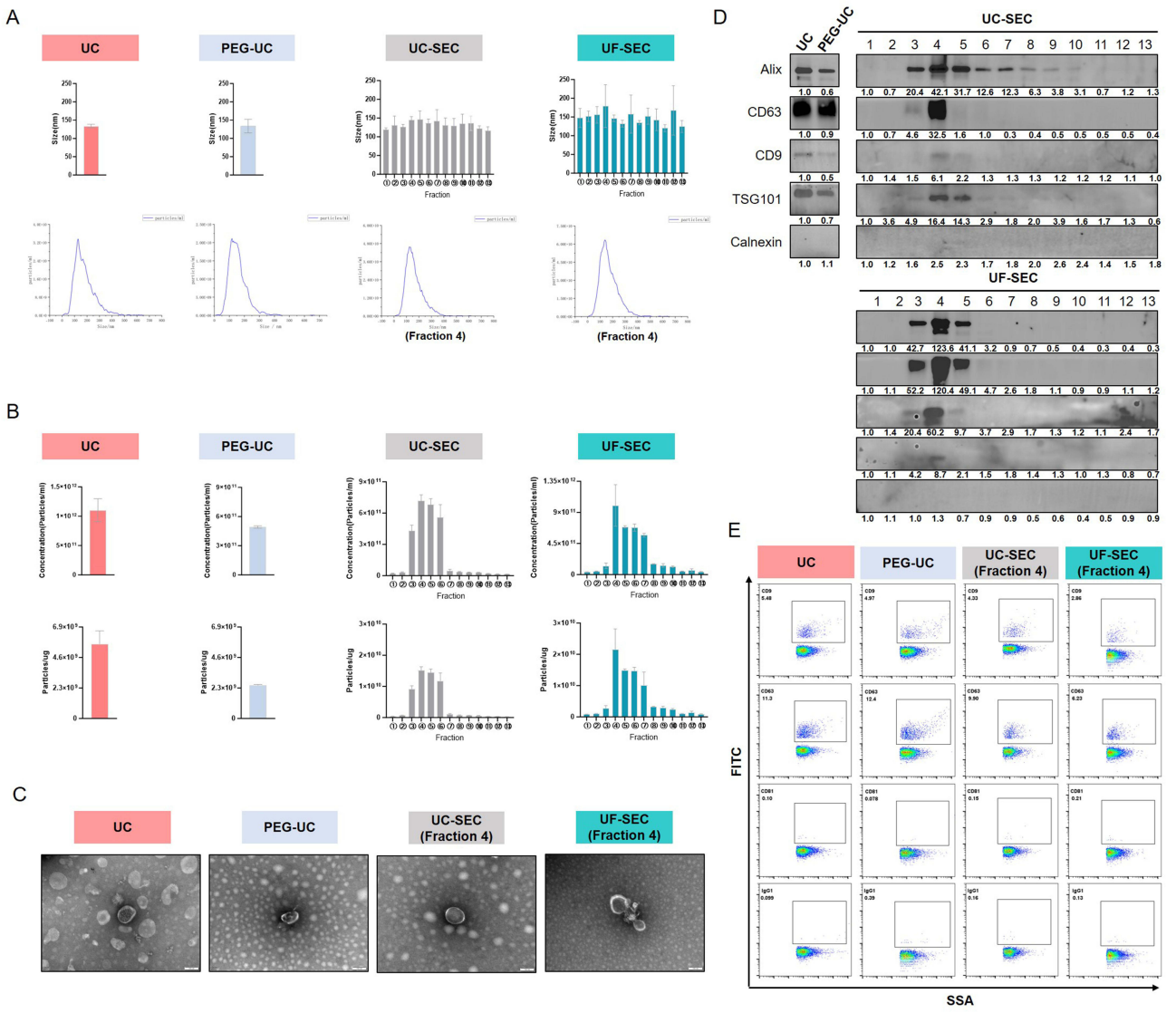

Figure 1 Characteristics of gsEVs isolated by four methods. (**A**) The size of gsEVs were detected by NTA (Upper panel: statistical charts of particle size; Lower panel: representative images of particle size distribution). (**B**) The concentration of gsEVs particles (Upper panel: particle number per milliliter was detected by NTA; Lower panel: particle number per microgram of protein). (**C**) The morphological characteristics of gsEVs were detected by TEM. (**D**) The sEVs markers (Alix, CD63, CD9 and TSG101) and the non-sEVs marker (Calnexin) were detected by Western blotting. In the UC and PEG-UC methods, 20 μg of protein was loaded; in the UC-SEC and UF-SEC methods, 20 μL of each fraction was loaded. (**E**) The membrane markers of sEVs (CD9, CD63 and CD81) were detected by NanoFCM.

results showed that the UC method identified the largest number of proteins (1772 ± 197), followed by UC-SEC (1572 ± 133) and UF-SEC (1448 ± 111) (Figure 2A). Principal component analysis (PCA) indicated that proteomic profiles of gsEVs isolated by UC and UC-SEC were similar, while profiles from UF-SEC were distinct from both (Figure 2B). Additionally, gsEVs from different individuals exhibited clear and well-defined clustering. A Venn diagram categorizing the proteins identified across all samples revealed that 1529 core proteins were identified in the UC method, 1274 in UC-SEC, and 1074 in UF-SEC. A total of 921 core proteins were detected in gsEVs isolated by all three methods (Figure 2C). This may be due to the UF-SEC method's inability to completely remove high-abundance contaminating proteins, which hindered the detection of low-abundance proteins.

Furthermore, the proteomic profiles of gsEVs isolated by the three methods were analyzed. Initially, the identified gsEV proteins were cross-referenced with the ExoCarta database, a web-based repository of characterized sEV cargo.[30,31] The analysis revealed that 82.15% (1256/1529) of the core proteins identified using the UC method aligned with the ExoCarta database. Similarly, 82.81% (1055/1274) and 84.08% (903/1074) of the core proteins identified by

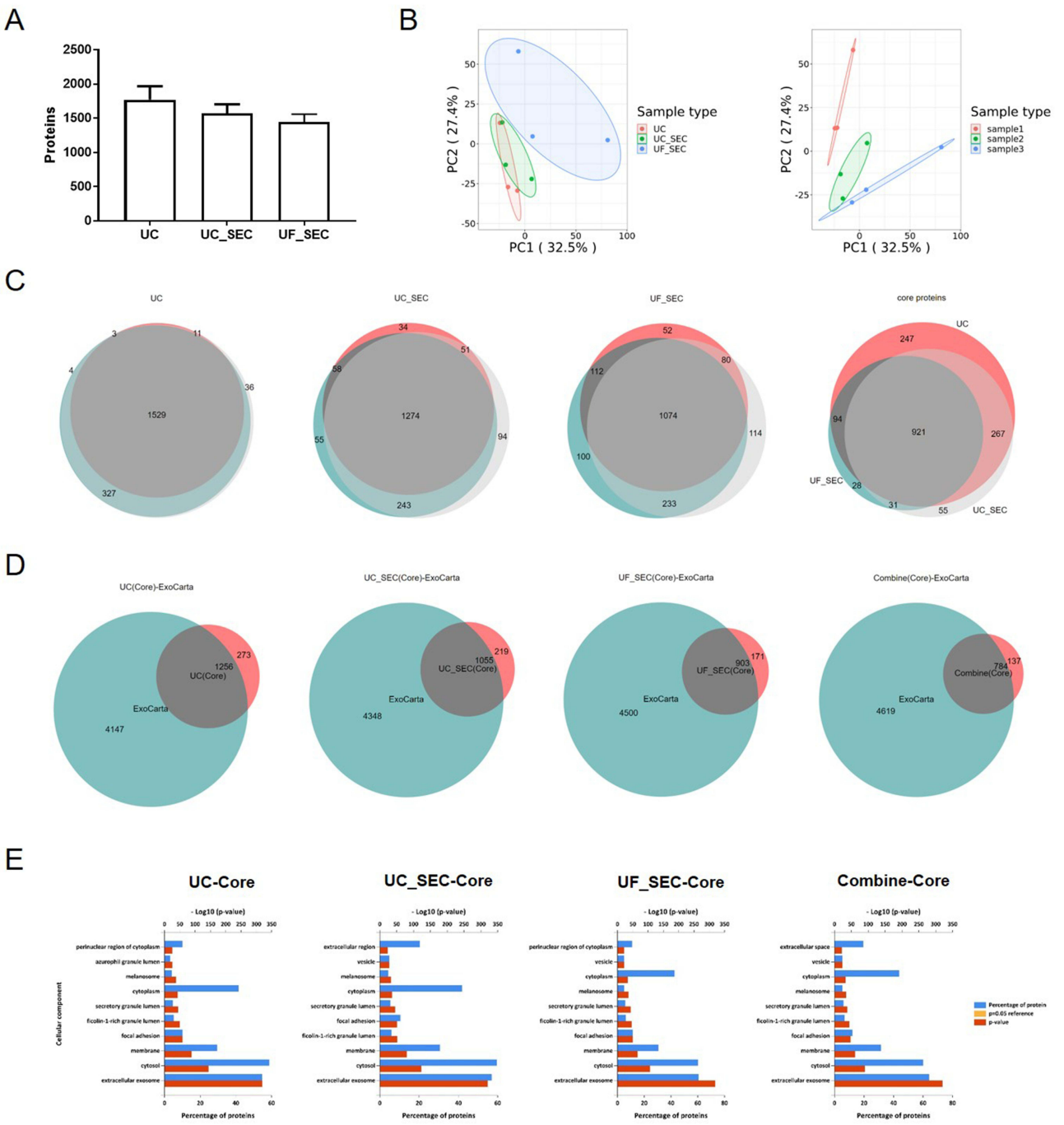

Figure 2 Proteomic analysis of gsEVs isolated by three methods. (**A**) The number of gsEVs proteins identified by LC-MS/MS in three methods. (**B**) Principal component analysis (PCA) of gsEVs proteins for three methods or three samples. (**C**) The core proteins of each method and all methods were analyzed using a Venn diagram. (**D**) The core proteins of gsEVs were matched with proteins in the ExoCarta database. (**E**) The core proteins of gsEVs were analyzed using GO cellular component annotation and listed according to *p-value*.

the UC-SEC and UF-SEC methods, respectively, were also matched. Furthermore, 85.12% (784/921) of the core proteins identified across all three methods were found to be consistent with ExoCarta-reported sEVs proteins (Figure 2D). To assess the isolation efficiency of the three methods, the ExoCarta top 100 protein list was utilized. In line with previous results, gsEVs isolated by the UC method showed the highest percentage of ExoCarta Top 100 proteins (87%), followed by UC-SEC (82%) and UF-SEC (76%) (Supplementary Figure 3A). A comparison of the proteins identified in gsEVs from all three methods was also made with the Vesiclepedia database, a compendium of

https://doi.org/10.2147/IJN.S516605

RNA, proteins, lipids, and metabolites in sEVs.[32] As expected, gsEVs isolated by the UC method matched the highest number of proteins in the Vesiclepedia database and identified the largest proportion of Vesiclepedia Top 100 proteins (Supplementary Figure 3B). These findings indicate that the UC method resulted in the highest quantity and proportion of identified sEV proteins.

Additionally, GO analysis of cellular components was performed to annotate the proteins detected by all three isolation methods. The top 10 most statistically significant items were ranked based on their p-values and protein percentages. The results showed that the majority of gsEVs proteins identified by all three methods were predominantly localized to the "extracellular exosome" compartment (Figure 2E). These findings demonstrate that gsEVs can be successfully isolated using all three methods.

Moreover, proteins identified exclusively by a single method were categorized as "unique proteins". The unique proteins detected by each method were also compared with the ExoCarta database. Notably, over 70% of the unique proteins identified by each method were found in the ExoCarta database. Consistently, the UC method identified the largest number of unique proteins matching with the ExoCarta database among the three methods (Supplementary Figure 4A). GO analysis was further applied to classify the unique proteins detected by the three methods. The results revealed that the unique proteins identified by the UC method were predominantly enriched in the "extracellular exosome" category, whereas the unique proteins detected by UC-SEC and UF-SEC were more concentrated in the "cytosol" (Supplementary Figure 4B). These findings suggest that the UC method provided higher purity gsEVs and improved the proteomic analysis of gsEVs.

TFF2 Is Highly Expressed in gsEVs

Based on quantitative proteomics, we further explored the significance of the highly expressed proteins in gsEVs. The top 20 proteins identified by each method were first compiled. To identify novel and specific biomarkers of gsEVs, these highly abundant proteins were compared with human stomach proteins from the Human Protein Atlas database (Supplementary Table 1). Among the core proteins identified by all three methods, two proteins, TFF2 and AKR1B10, matched with human stomach tissue proteins (Figure 3A). To further validate their tissue specificity, gene expression data were retrieved from the GEPIA database (Gene Expression Profiling Interactive Analysis, http://gepia.cancer-pku.cn/),[33] which integrates data from TCGA and GTEx projects. (Supplementary Figure 5) shows their expression profiles across various normal tissues, confirming their preferential expression in the stomach. This suggests that TFF2 is specifically expressed in stomach tissue. Furthermore, the expression of TFF2 in gsEVs was analyzed using WB. TFF2 was detected in gsEVs isolated by all three methods (Figure 3B). These results indicate that TFF2 is highly expressed in gsEVs and may serve as a potential specific biomarker for gsEVs.

TFF2 Is Specifically Expressed in sEVs Derived From Gastric Mucosal Cells

TFFs, including TFF1, TFF2, and TFF3, are a family of small secretory proteins that play crucial roles in protecting and repairing the gastrointestinal tract.[34] TFF2 is predominantly co-expressed with mucin MUC6 in the gastric epithelium and Brunner's glands of the duodenum.[35] Given that TFF2 is a small secreted peptide, we aimed to confirm whether the TFF2 detected by LC-MS/MS and WB originated from soluble proteins in the supernatant of UC or specifically from gsEVs. To investigate this, a gastric mucosal cell line overexpressing TFF2 (GES1-TFF2-OE) and a control line (GES1-NC) were established (Supplementary Figure 6A). sEVs were then isolated from the cell culture medium using the UC method. NTA, TEM, and WB confirmed the successful isolation of sEVs (Figure 4A–C). Quantitative analysis of total protein (Supplementary Figure 6B) revealed that TFF2 was predominantly expressed in sEVs rather than in the supernatant of UC (Figure 4C), suggesting that TFF2 is specifically expressed in sEVs derived from gastric mucosal cells. Additionally, sEVs markers, including CD9, CD63, and CD81, were detected by flow cytometry using bead binding. These markers were present in sEVs derived from both GES1-NC and GES1-TFF2-OE cells, with a positive ratio below 10% (Figure 4D). In comparison to the isotype, the expression level of TFF2 was significantly higher in bead-bound sEVs, with a positive ratio of approximately 25% (Figure 4E). These findings suggest that TFF2 could serve as a promising and specific biomarker for sEVs derived from gastric cells.

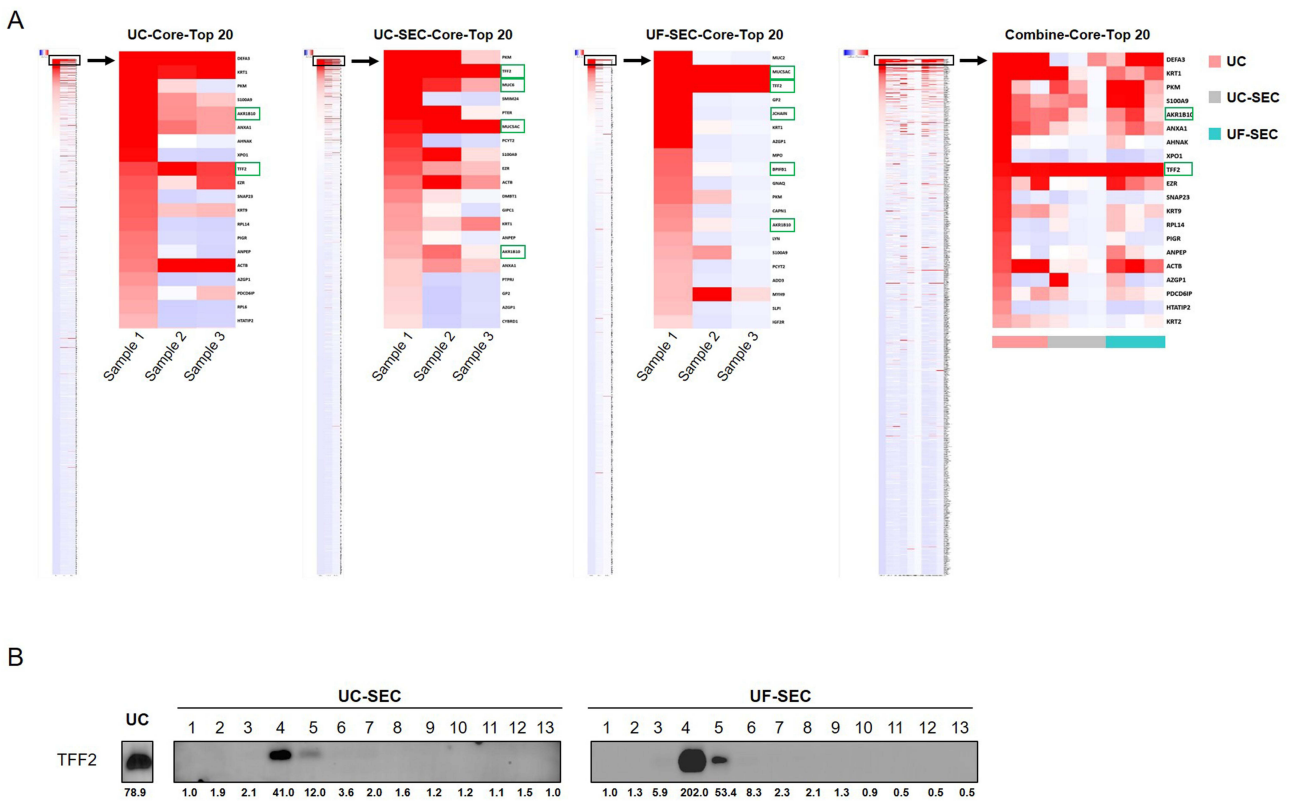

Figure 3 TFF2 is highly expressed in gsEVs. (**A**) The expression levels of identified core proteins in each method were presented using a heatmap. The green box highlights stomach tissue proteins in the Human Protein Atlas database. (**B**) The expression level of TFF2 was detected in gsEVs by Western blotting.

TFF2 Is Specifically Expressed in gsEVs Derived From Mice and Humans

The specific expression of TFF2 in sEVs was further validated in vivo. First, GJ from both mice and humans was collected, and gsEVs were isolated using the UC method. NTA, TEM, and WB results confirmed the successful isolation of gsEVs from both mice and humans (Figure 5A–D). Compared to the quantitative results for total protein (Supplementary Figure 7A and B), TFF2 was predominantly expressed in gsEVs rather than in the UC supernatant of GJ (Figure 5C and D). Additionally, the expression level of TFF2 was also assessed in gsEVs derived from human sources. Using bead binding flow cytometry, the expression level of TFF2 in human gsEVs was found to be significantly higher than in the isotype control. As observed in NanoFCM, CD63-positive beads showed the highest percentage, followed by CD9-positive beads, while CD81-positive beads were almost undetectable (Figure 5E and F). Immunogold labeling combined with TEM further confirmed the positive expression of CD63, the intracellular protein Syntenin-1, and the secretory protein TFF2 in human gsEVs, relative to the control. Consistent with prior studies that identified Syntenin-1 as a universal intraluminal biomarker in EVs,[27] our findings demonstrated a significantly stronger immunoreactive signal for TFF2, emphasizing its potential as a distinctive marker in gsEVs (Figure 5G). These results confirm that TFF2 is specifically expressed in gsEVs derived from both mice and humans, suggesting that TFF2 may serve as a potential specific biomarker for sEVs derived from GJ.

TFF2 as a Potential Specific Biomarker of gsEVs

To further assess the specificity of TFF2 as a biomarker for gsEVs, sEVs derived from GJ, intestinal juice, and plasma were analyzed. GJ, intestinal juice, and plasma were collected from mice, and sEVs were isolated by the UC method. NTA, TEM, and WB analyses showed that sEVs were successfully isolated from intestinal juice and plasma (Figure 6A–C). The expression level of TFF2 were significantly higher in gsEVs compared to sEVs derived from intestinal juice and plasma (Figure 6C and Supplementary Figure 8A). Additionally, the expression of TFF2 was also evaluated in human-derived sEVs from GJ, intestinal juice, and plasma. Consistent with the results in mice, TFF2 was specifically expressed in gsEVs and not in sEVs derived from

https://doi.org/10.2147/IJN.S516605

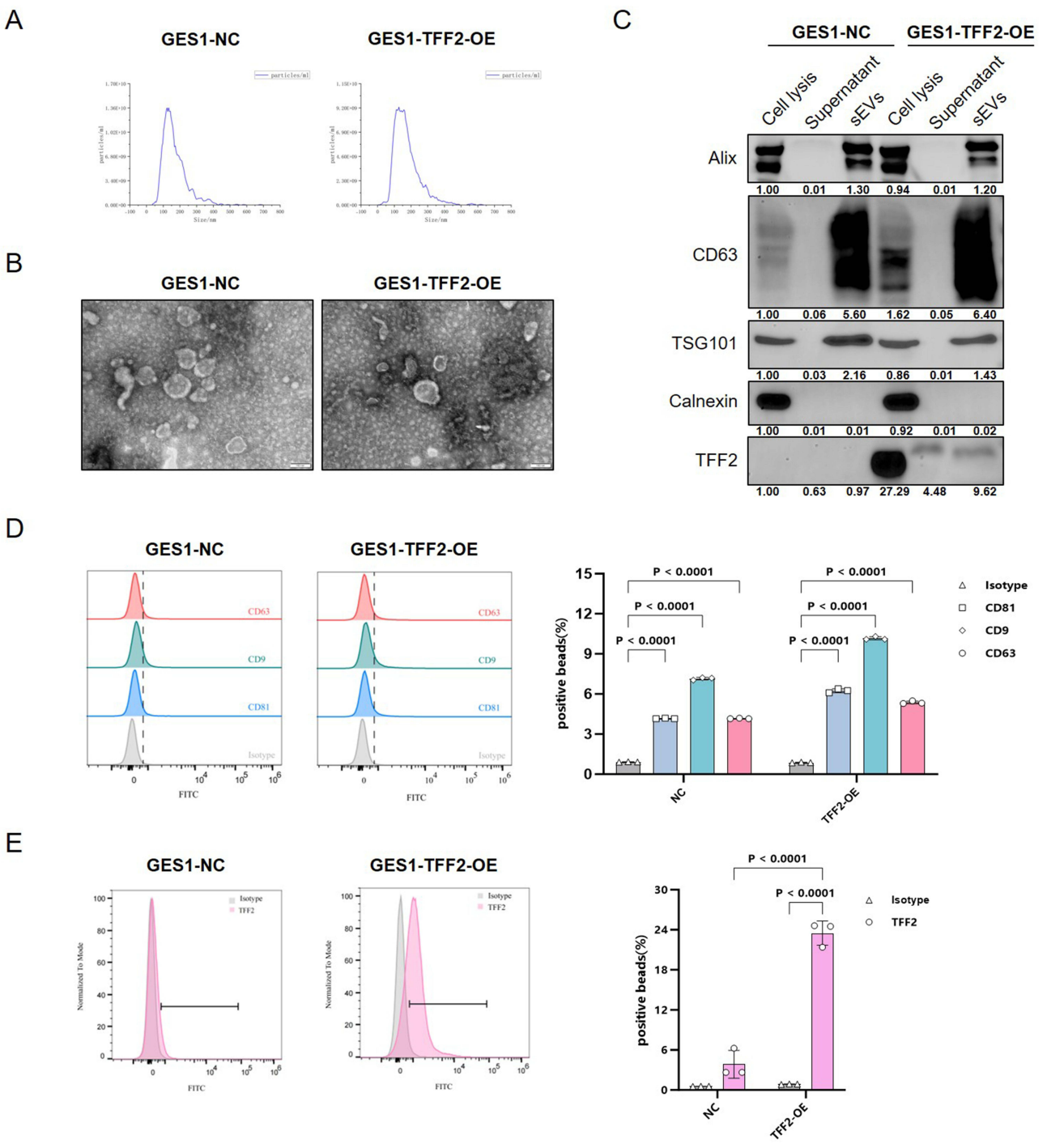

Figure 4 TFF2 is specifically expressed in sEVs derived from gastric mucosal cells. (**A**) The particle size distribution of sEVs derived from gastric mucosal cells GES1-NC and GES1-TFF2-OE. (**B**) The morphological characteristics of cell culture medium-derived sEVs were observed by TEM. (**C**) The sEVs markers (Alix, CD63 and TSG101), the non-sEVs marker (Calnexin), and TFF2 were detected in Cell lysis, ultracentrifugation supernatant, and sEVs. (**D** and **E**) The expression levels of membrane markers of sEVs (CD9, CD63, and CD81) and TFF2 were detected by bead-bound flow cytometry in sEVs derived from GES1-NC and GES1-TFF2-OE cells.

intestinal juice or plasma (Figure 6D–F and Supplementary Figure 8B). These findings indicate that TFF2 may be a promising and specific biomarker for gsEVs.

Potential Functions of TFF2 in gsEVs

Given the specific expression of TFF2 in gsEVs, we further explored its potential functions through multi-omics analysis. Initially, transcriptome analysis was performed on gastric mucosa cells overexpressing TFF2. Compared to the control

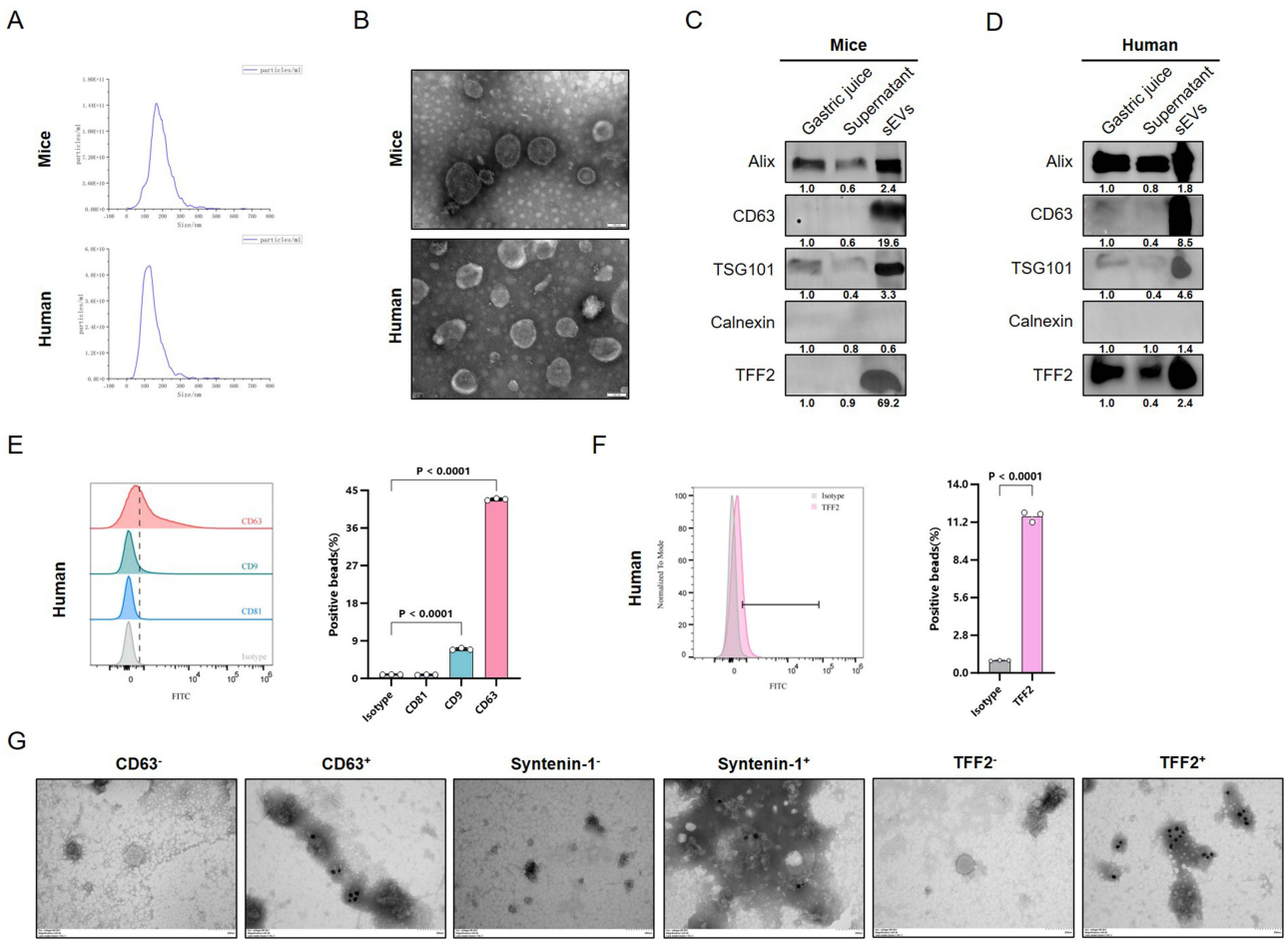

Figure 5 TFF2 is specifically expressed in sEVs derived from GJ. (**A**) The particle size distribution of sEVs derived from GJ in mice and human. (**B**) The morphological characteristics of gsEVs derived from mice and humans were observed by TEM. (**C**) The sEVs markers, non-sEVs marker, and TFF2 were detected in GJ, ultracentrifugation supernatant, and gsEVs derived from mice. (**D**) The sEVs markers, non-sEVs marker, and TFF2 were detected in GJ, ultracentrifugation supernatant, and gsEVs derived from human. (**E** and **F**) The expression levels of membrane markers of sEVs (CD9, CD63 and CD81) and TFF2 was detected by bead-bound based flow cytometry in human gsEVs. (**G**)The expression levels of sEV markers, including CD63, Syntenin-1, and TFF2, were analyzed in human gsEVs using immunogold labeling and TEM.

cells (GES1-NC), 139 genes were found to be upregulated, while 135 genes were downregulated (Figure 7A). GO enrichment analysis indicated that the differentially expressed genes (DEGs) were primarily associated with positive regulation of the MAPK cascade and chemokine-mediated signaling pathways in the biological process (BP) category. In molecular function (MF) analysis, the DEGs were predominantly linked to CXCR chemokine receptor binding and chemokine receptor binding (Figure 7B). KEGG signaling pathway analysis revealed significant enrichment in cancer-related pathways, including the GC and Wnt signaling pathways, as well as pathways associated with inflammation, such as the NF-kappa B signaling pathway and cytokine-cytokine receptor interaction (Figure 7C). Protein-protein interaction (PPI) network analysis identified key genes associated with cancer and inflammation, such as WNT2, WNT7B, LGR5, IL8, CXCL2, CCL20, and CXCR7 (Figure 7D). These transcriptomic results suggest that TFF2 may be involved in cancer and inflammation within gastric mucosa cells.

Since proteins are the key molecules that mediate biological functions, we further investigated the role of TFF2 in sEVs through proteomic analysis. Compared to sEVs derived from GES1-NC cells, 85 proteins were upregulated, and 132 proteins were downregulated in sEVs derived from GES1-TFF2-OE cells (Figure 7E). GO enrichment analysis showed that the differentially expressed proteins (DEPs) were primarily involved in the regulation of gastric acid secretion and the positive regulation of interleukin-8 production in biological processes (BPs). In molecular function (MF) analysis, the DEPs were mainly associated with transmembrane transporter activity and signaling receptor activity (Figure 7F). KEGG signaling pathway analysis revealed that the DEPs were significantly enriched in immune-related

https://doi.org/10.2147/IJN.S516605

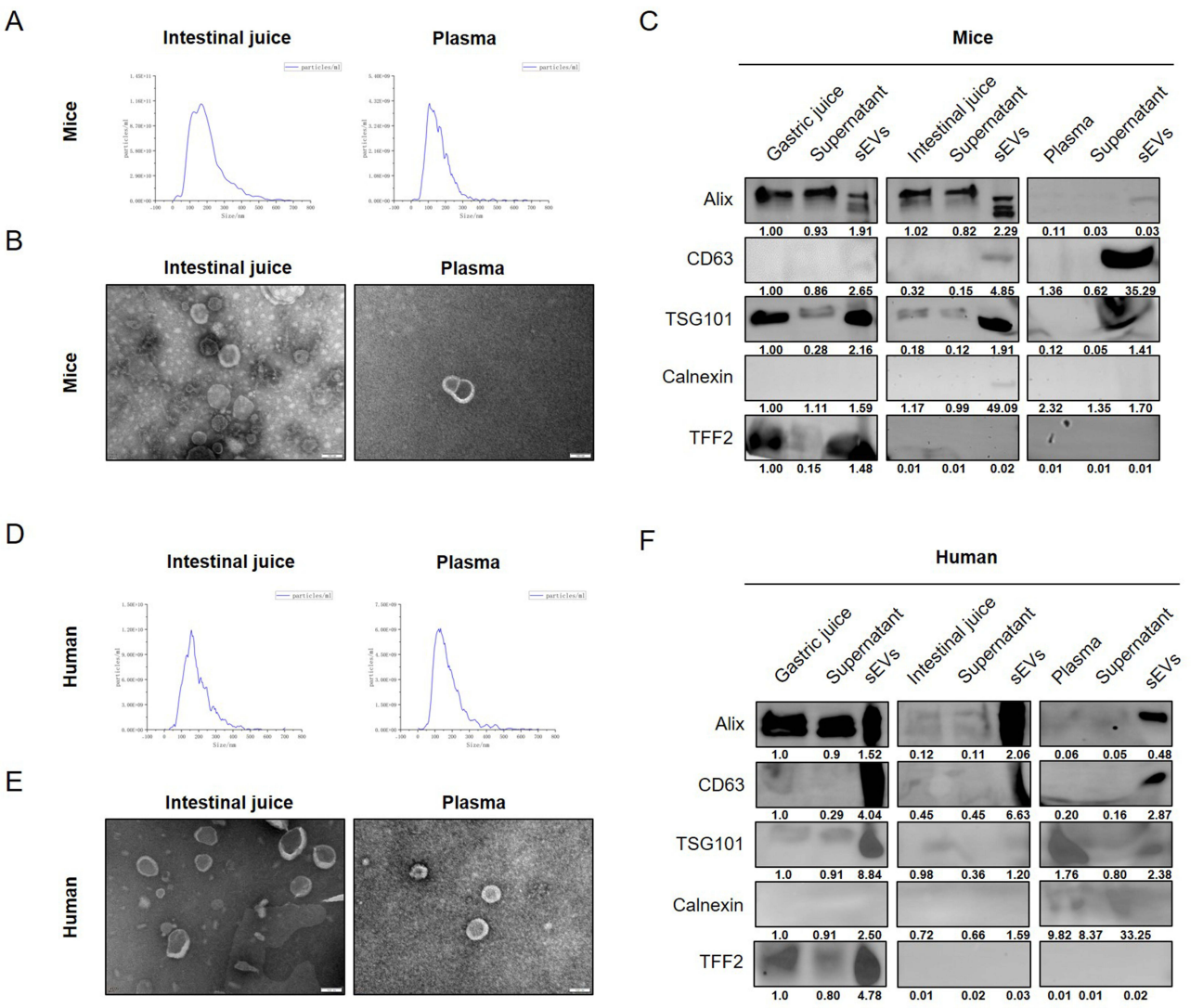

Figure 6 TFF2 is a potential specific biomarker of gsEVs. (**A**) The particle size distribution of sEVs derived from intestinal juice and plasma in mice. (**B**) The morphological characteristics of intestinal juice and plasma-derived sEVs in mice were observed by TEM. (**C**) The sEVs markers, non-sEVs marker, and TFF2 were detected in three types of bodily fluids, ultracentrifugation supernatant, and sEVs derived from mice. (**D**) The particle size distribution of sEVs derived from intestinal juice and plasma in humans. (**E**) The morphological characteristics of intestinal juice and plasma-derived sEVs in human were detected by TEM. (**F**) The sEVs markers, non-sEVs marker, and TFF2 were detected in three types of bodily fluids, ultracentrifugation supernatant, and sEVs derived from humans.

pathways (Figure 7G). PPI network analysis showed that key proteins were predominantly associated with ribosomal components, including RPS23, RPS2, RPS4X, RPS16, RPS15A, and RPS17 (Figure 7H). These findings from the proteomic analysis indicate that TFF2 may play a role in immune response, transmembrane transporter activity, and ribosome function in gastric mucosa-derived sEVs. Furthermore, five molecules (WNT7B, HSPA1A, TMEM178B, LOX, ASNS) exhibited differential expression in both transcriptomic and proteomic analyses, and were primarily involved in cancer and immunity.

Given that TFF2 is specifically expressed in gsEVs and the proteomic analysis suggests its involvement in transmembrane transporter activity, we next investigated whether TFF2 affects the secretion of sEVs. The particle number of sEVs per cell was measured using NTA and a cell counter in both GES1-NC and GES1-TFF2-OE cells. The results showed no significant differences between the two groups (Supplementary Figure 9A). Since the particles counted by NTA may not necessarily represent authentic sEVs, we further analyzed the number of particles per microgram of protein using both NTA and BCA assays, which also revealed no significant differences (Supplementary Figure 9B). These preliminary results suggest that TFF2 may not have a significant impact on the secretion of sEVs.

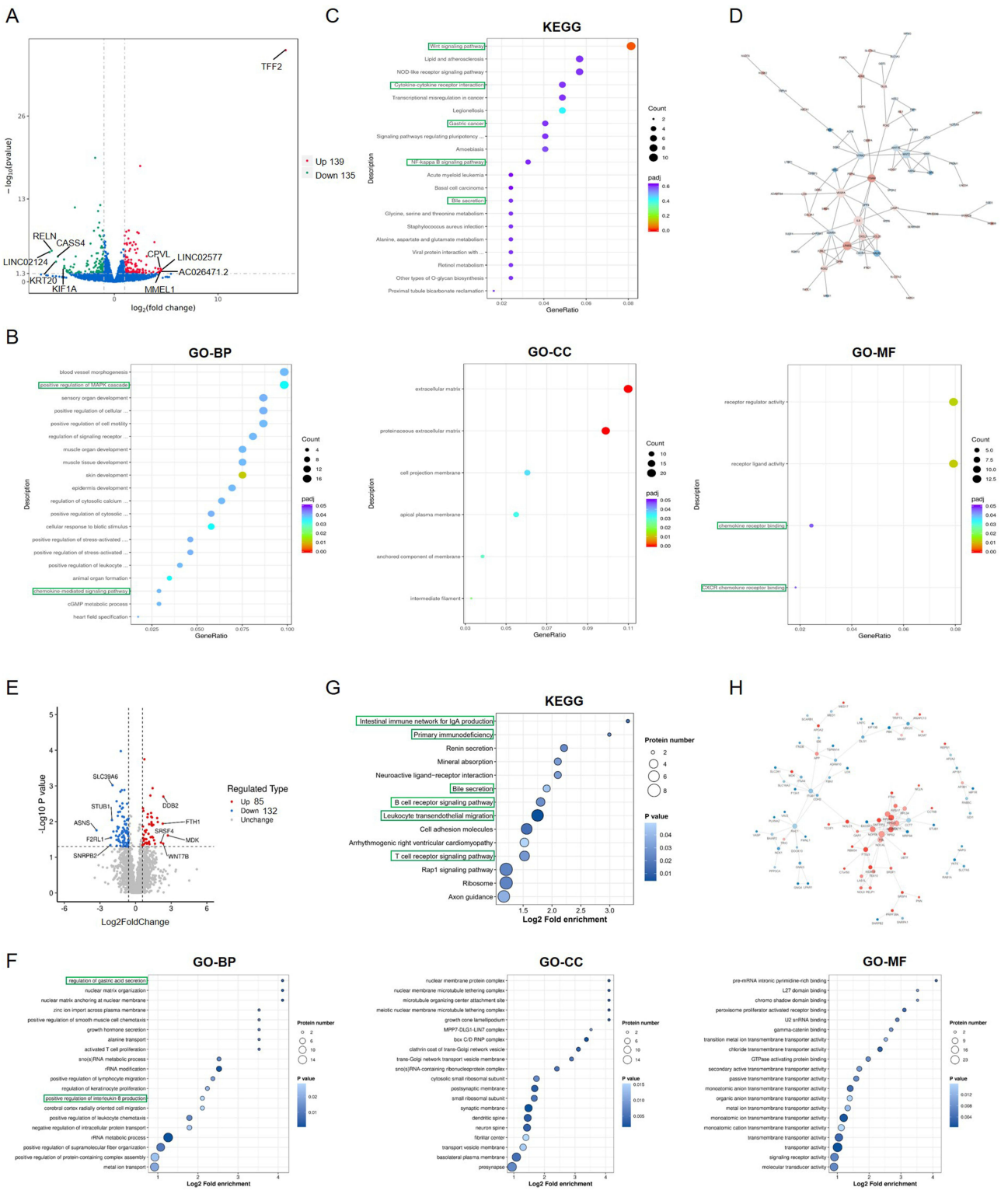

Figure 7 Multi-omics analysis of the function of gsEVs-carried TFF2. (**A**) The different expression genes (DEGs) in GES1-NC and GES1-TFF2-OE cells from transcriptomic analysis. (**B**–**D**) GO enrichment analysis, KEGG signaling pathway analysis, and PPI network analysis of DEGs in GES1-NC and GES1-TFF2-OE cells. (**E**) The DEPs in sEVs derived from GES1-NC and GES1-TFF2-OE cells by proteomic analysis. (**E**–**H**) GO enrichment analysis, KEGG signaling pathway analysis, and PPI network analysis of DEPs in sEVs derived from GES1-NC and GES1-TFF2-OE cells.

https://doi.org/10.2147/IJN.S516605

Discussion

GsEVs, derived from GJ, are in direct contact with gastric tissue, suggesting their significant potential for diagnosing gastric diseases. Effective isolation of gsEVs is essential for functional research. Currently, the most commonly used methods for isolating gsEVs are UC[36,37] and precipitation,[19,20] though research on isolation methods for gsEVs remains limited. UC is a widely adopted technique for isolating sEVs, yet it struggles to remove certain lipoprotein particles, such as high-density lipoprotein (HDL), especially from plasma samples.[38,39] While precipitation achieves the highest particle yield, it often results in a higher presence of non-sEVs particles.[22] Other common isolation methods, such as SEC and UF, also present limitations. Although SEC is straightforward and can isolate relatively pure sEVs, it fails to differentiate sEVs from similarly sized particles and suffers from limited input volume and dilution effects during elution.[22] The UF method or precipitation with PEG can increase the yield of sEVs but tends to produce lower purity final preparations.[40] As the key challenge in isolating sEVs lies in balancing yield and purity, many researchers suggest combining different isolation methods to enhance efficiency.[41–43] In this study, we employed UC, PEG precipitation, SEC, and UF, both individually and in combination, to improve gsEV isolation efficiency. The results showed that UC achieved the highest particle yield, while the PEG-UC method resulted in the lowest yield.

The number of particles per microgram of protein has been established as a reliable indicator of EV purity in previous studies.[44] Our findings indicated that the UC-SEC and UF-SEC methods yielded the highest amounts of high-purity gsEVs, with the UC method producing fewer particles and PEG-UC being the least effective. However, TEM analysis revealed that gsEVs isolated by the UC method were relatively pure, whereas those isolated by the other methods contained more non-sEV particles. Considering both yield and purity, we conclude that the UC method is more suitable for isolating gsEVs.

Proteomic analysis further supported the UC method's superiority in isolating gsEVs, as it identified the highest number of proteins. When the core proteins from each method were compared against the ExoCarta database, over 80% of the core proteins from each method matched ExoCarta entries, with UC identifying the largest number of sEV-associated proteins. Similar comparisons using the Vesiclepedia database also revealed that gsEVs isolated by UC matched the most proteins. Additionally, when the unique proteins identified by each method were compared against the ExoCarta database, UC again identified the greatest number of sEV-associated proteins. GO analysis of the core and unique proteins showed that proteins identified across all methods were predominantly enriched in the "extracellular exosome" category. Unique proteins identified by UC were also mainly enriched in "extracellular exosome", whereas proteins unique to the UC-SEC and UF-SEC methods were primarily associated with the "cytosol". These findings suggest that gsEVs isolated by UC not only contain the largest number of proteins but also exhibit the highest proportion of sEV-associated proteins. Our study provides a novel approach for gsEV isolation, particularly for downstream proteomics analysis.

Tetraspanins, including CD9, CD81, and CD63, are widely used as markers to characterize sEVs. In this study, all three of these membrane markers were detected in gsEVs by NanoFCM, although their expression levels varied. CD63-positive particles exhibited the highest percentage, followed by CD9-positive particles, while CD81-positive particles were almost undetectable These findings suggest that the expression levels of common sEV biomarkers in gsEVs are heterogeneous. Previous studies have reported similar heterogeneity in the expression of these markers across sEVs from different samples,[27] which could be attributed to variations in the loading efficiency of membrane proteins in EVs, as well as the diverse cellular or tissue origins of the vesicles. Our earlier work also found that in sEVs derived from pleural effusion, CD81 was the most prominent marker, whereas CD63 was the least abundant.[14] This variability highlights the need to identify specific and efficient biomarkers for gsEVs. It has been established that sEVs from different tissues and biofluids have distinct biomarkers. For example, Ldb3 has been identified as a potential marker for cardiac sEVs, showing almost exclusive detection in the neonatal rat heart compared to other tissues, and is particularly prominent in cardiomyocytes relative to cardiac fibroblasts.[28] Similarly, PODXL, OCT4, Dnmt3a, and LIN28A are recognized as specific markers for PSC-derived sEVs.[29] In our study, we found that TFF2 could serve as a potential specific biomarker for gsEVs. Proteomic analysis revealed high expression of TFF2 in gsEVs isolated by all methods. We further validated the specificity of TFF2 in gsEVs through in vitro and in vivo experiments. In vitro, our results demonstrated that, compared to the total protein quantification, TFF2 was primarily expressed in sEVs derived from the GES-1 cell culture

medium, rather than in the supernatant after UC. This suggests that TFF2 is specifically expressed in gastric mucosal cell-derived sEVs. We also observed that TFF2 was predominantly expressed in gsEVs derived from both mouse and human GJ, rather than in the GJ supernatant after UC under physiological conditions. Moreover, flow cytometry using bead binding and immunogold-labeled TEM confirmed the presence of TFF2 in gsEVs. These results showed that the expression of TFF2 was significantly higher in gsEVs from GES-1 cells and human GJ compared to the control. Notably, TFF2 expression was even higher than that of Syntenin-1, another known intraluminal biomarker of EVs. Our findings thus provide strong evidence that TFF2 is specifically expressed in gastric cell-derived sEVs. Furthermore, TFF2 was detected in gsEVs but not in sEVs derived from intestinal juice or plasma from both mice and humans, suggesting that TFF2 could serve as a promising and specific biomarker for gsEVs.

To investigate the potential function of TFF2 in gsEVs, we conducted multi-omics analysis on TFF2-overexpressing gastric mucosa cells and their derived sEVs. Transcriptome analysis revealed that differentially expressed genes (DEGs) were predominantly enriched in cancer-related signaling pathways, such as GC and Wnt signaling, as well as inflammation-related pathways, including MAPK, JNK, NK-kappa B, and chemokine-mediated signaling pathways. Furthermore, key DEGs were focused on cancer and inflammation-associated genes, such as WNT2, WNT7B, LGR5, IL8, CXCL2, CCL20, and CXCR7. As part of the TFF family, TFF2 is mainly expressed in the stomach and plays a crucial role in maintaining the integrity of the gastric mucosa, potentially inhibiting tumorigenesis in the stomach. Pathologically, TFF2 expression is abnormal in various conditions, including stone diseases, chronic inflammation, and multiple metaplastic and neoplastic epithelia. Notably, TFF2 is highly expressed in spasmolytic polypeptide-expressing metaplasia (SPEM), a recognized precancerous lesion of the stomach.[35] Consistently, transcriptome analysis in this study indicated that TFF2 is involved in cancer and inflammation in gastric mucosa cells. Additionally, proteomic analysis revealed that DEPs between sEVs derived from GES1-NC and GES1-TFF2-OE cells were enriched in bile acid and gastric acid secretion pathways, transmembrane transporter activity, and immune-related signaling pathways, such as IL-8 production and T cell and B cell receptor signaling. Bile acids and gastric acids are known to induce chronic inflammation and contribute significantly to gastrointestinal diseases, including metaplasia. For instance, deoxycholic acid-stimulated macrophage-derived exosomes promote TFF2 and GSII lectin expression in the stomach, markers of SPEM.[45] TFF2-deficient mice exhibit reduced gastric mucosal thickness, decreased proliferation rates, and increased gastric acid secretion, leading to heightened gastric ulceration following indomethacin treatment. These findings highlight the crucial physiological role of TFF2 in promoting mucosal healing by stimulating cellular proliferation and reducing gastric acid secretion.[46] Interestingly, DEPs were also enriched in transmembrane transporter activity, prompting us to explore whether TFF2 affects sEV secretion. However, our results showed no significant changes in the number of sEVs derived from TFF2-overexpressing gastric mucosa cells compared to control cells. Further research is needed to determine the exact role of TFF2 in sEVs secretion. Notably, the key DEPs were primarily associated with ribosomal proteins, such as RPS23, RPS2, RPS4X, RPS16, RPS15A, and RPS17, suggesting that TFF2 may influence ribosome function in gsEVs. However, the precise role of TFF2 in ribosomes requires further verification.

Additionally, five molecules (WNT7B, HSPA1A, LOX, ASNS, and TMEM178B) exhibited differential expression in both transcriptomic and proteomic analyses. Previous studies have highlighted the role of WNT7B in activating the Wnt/β-catenin signaling pathway.[47] Specifically, a positive feedback loop involving WNT7B-m6A-TCF7L2 has been shown to accelerate the progression and metastasis of GC.[48] HSPA1A, also known as heat shock protein 70 (HSP70), is typically expressed at low or undetectable levels in normal, unstressed cells. However, various tumor cell types overexpress HSPA1A on the plasma membrane, contributing to resistance against programmed cell death and promoting tumor progression.[49] Moreover, HSPA1A is released into the extracellular environment via exosomes, with tumor-derived exosomes being particularly enriched with HSPA1A,[50] in contrast to exosomes derived from normal 3T3 cells.[51] In this study, HSPA1A was found to be downregulated in TFF2-overexpressing gastric mucosa cells and sEVs, suggesting that TFF2 may play a potential anti-cancer role in the stomach. Asparagine is known to be essential for cancer cell progression, and targeting asparagine has emerged as a potential anti-cancer strategy, with proven efficacy in leukemia therapy. However, targeting asparagine alone has limited therapeutic success due to stress-induced upregulation of asparagine synthase (ASNS), which allows cancer cells to maintain asparagine levels.[52] ASNS has been shown to be overexpressed in certain cancers, where it supports cell proliferation, enhances chemoresistance, promotes metastasis, and contributes to the tumor microenvironment.[53] The lysyl oxidase (LOX) family,

which includes LOX and four LOX-like proteins (LOXL1, LOXL2, LOXL3, and LOXL4), plays a crucial role in extracellular matrix (ECM) remodeling and collagen cross-linking.[54] LOX is upregulated under hypoxic conditions and contributes to tumor cell invasion and metastasis.[55] Moreover, LOX is involved in tumor microenvironment remodeling and could serve as a potential therapeutic target for cancer treatment.[56] Transmembrane protein 178B (TMEM178B) is predicted to be an integral membrane component, though its functions remain understudied. These findings suggest that TFF2-enriched gsEVs may influence pathways related to cancer progression and inflammation. However, it is important to note that our study did not include tumor-derived samples, meaning that the proposed anti-cancer or immunomodulatory roles of TFF2 remain speculative. Further investigations using disease-specific specimens are required to validate these mechanistic insights.

These findings collectively suggest that gsEVs carrying TFF2 may not only serve as diagnostic markers but also play a role in the pathophysiological processes of gastric inflammation, mucosal repair, and potentially early gastric carcinogenesis. However, it is important to note that our study was conducted using samples from healthy individuals. As such, the relevance of TFF2-enriched gsEVs in disease contexts remains hypothetical and necessitates further investigation using clinical specimens from patients with GC or gastritis.

Conclusion

In summary, the UC method has proven to be effective for isolating sEVs from GJ, particularly for subsequent proteomic analysis. TFF2 emerges as a potential specific biomarker for gsEVs, and gsEVs carrying TFF2 may contribute to anti-cancer mechanisms in the stomach. TFF2 plays a crucial role in maintaining the integrity of the gastric mucosa and suppressing tumorigenesis in the stomach. Our results suggest that TFF2 may be involved in intercellular communication and exert its effects by being incorporated into gsEVs. However, there are several limitations to the current study. First, the roles of TFF2 in gsEVs were examined primarily through multi-omics analysis, and its precise functions need to be further validated through in vitro and in vivo experiments. Second, while we propose TFF2 as a potential specific biomarker for gsEVs, it remains unclear whether TFF2 influences sEV secretion. Future research will focus on exploring the role of TFF2-enriched gsEVs, specifically their involvement in GC, gsEV secretion, and ribosome function.

Ethics Approval and Consent to Participate

The acquisition of all clinical samples was authorized by the Ethics Committee of the Third People's Hospital of Chengdu (2024-S-212), and informed consent was acquired from all volunteers involved in the study. All animal studies were conducted following the guidelines outlined in the China Public Health Service Guide for the Care and Use of Laboratory Animals. Mouse-related experiments and associated protocols received approval from the Ethics Committee of Southwest Jiaotong University Approval (Agreement No. SWJTU-2103-026). The study was conducted in accordance with the Declaration of Helsinki.

Funding

This study was funded by the foundation of Chengdu Municipal Science and Technology Bureau (2024-YF05-00853-SN), the Third People's Hospital of Chengdu Scientific Research Project (2023PI19), and the Third People's Hospital of Chengdu Clinical Research Program (CSY-YN-03-2024-014).

Disclosure

The authors confirm that they have no conflicts of interest to disclose in this work.

References

1. Zullo A, Annibale B, Dinis-Ribeiro M, et al. Gastric juice analysis in clinical practice: why, how, and when. The experience with EndoFaster. *Eur J Gastroenterol Hepatol*. 2024;36(3):264–270. doi:10.1097/MEG.0000000000002704
2. Martinsen TC, Bergh K, Waldum HL. Gastric juice: a barrier against infectious diseases. *Basic Clin Pharmacol Toxicol*. 2005;96(2):94–102. doi:10.1111/j.1742-7843.2005.pto960202.x
3. Martinsen TC, Fossmark R, Waldum HL. The phylogeny and biological function of gastric juice-microbiological consequences of removing gastric acid. *Int J Mol Sci*. 2019;20(23):6031. doi:10.3390/ijms20236031

4. Vasapolli R, Ailloud F, Suerbaum S, et al. Intraprocedural gastric juice analysis as compared to rapid urease test for real-time detection of Helicobacter pylori. *World J Gastroenterol*. 2023;29(10):1638–1647. doi:10.3748/wjg.v29.i10.1638
5. Zullo A, Germanà B, Galliani E, et al. Real-time determination of gastric juice pH with EndoFaster(R) for atrophic gastritis assessment. *Dig Liver Dis*. 2022;54(12):1646–1648. doi:10.1016/j.dld.2022.06.014
6. Si YT, Xiong XS, Wang JT, et al. Identification of chronic non-atrophic gastritis and intestinal metaplasia stages in the Correa's cascade through machine learning analyses of SERS spectral signature of non-invasively-collected human gastric fluid samples. *Biosens Bioelectron*. 2024;262:116530. doi:10.1016/j.bios.2024.116530
7. Felipez N, Montori S, Mendizuri N, et al. The human gastric juice: a promising source for gastric cancer biomarkers. *Int J Mol Sci*. 2023;24 (11):9131. doi:10.3390/ijms24119131
8. Welsh JA, Goberdhan DC, O'Driscoll L, et al. Minimal information for studies of extracellular vesicles (MISEV2023): from basic to advanced approaches. *J Extracell Vesicles*. 2024;13(2):e12404. doi:10.1002/jev2.12404
9. van Niel G, D'Angelo G, Raposo G. Shedding light on the cell biology of extracellular vesicles. *Nat Rev Mol Cell Biol*. 2018;19(4):213–228. doi:10.1038/nrm.2017.125
10. Karimi N, Cvjetkovic A, Jang SC, et al. Detailed analysis of the plasma extracellular vesicle proteome after separation from lipoproteins. *Cell Mol Life Sci*. 2018;75(15):2873–2886. doi:10.1007/s00018-018-2773-4
11. Li X, Yang L. Urinary exosomes: emerging therapy delivery tools and biomarkers for urinary system diseases. *Biomed Pharmacother*. 2022;150:113055. doi:10.1016/j.biopha.2022.113055
12. Han P, Bartold PM, Ivanovski S. The emerging role of small extracellular vesicles in saliva and gingival crevicular fluid as diagnostics for periodontitis. *J Periodontal Res*. 2022;57(1):219–231. doi:10.1111/jre.12950
13. Li C, Qin T, Jin Y, et al. Cerebrospinal fluid-derived extracellular vesicles after spinal cord injury promote vascular regeneration via PI3K/AKT signaling pathway. *J Orthop Translat*. 2023;39:124–134. doi:10.1016/j.jot.2023.02.001
14. Yao X, Liao B, Chen F, et al. Comparison of proteomic landscape of extracellular vesicles in pleural effusions isolated by three strategies. *Front Bioeng Biotechnol*. 2023;11:1108952. doi:10.3389/fbioe.2023.1108952
15. Wang W, Jo H, Park S, et al. Integrated analysis of ascites and plasma extracellular vesicles identifies a miRNA-based diagnostic signature in ovarian cancer. *Cancer Lett*. 2022;542:215735. doi:10.1016/j.canlet.2022.215735
16. Del Rivero T, Milberg J, Bennett C, et al. Human amniotic fluid derived extracellular vesicles attenuate T cell immune response. *Front Immunol*. 2022;13:977809. doi:10.3389/fimmu.2022.977809
17. Kaddour H, Kopcho S, Lyu Y, et al. HIV-infection and cocaine use regulate semen extracellular vesicles proteome and miRNAome in a manner that mediates strategic monocyte haptotaxis governed by miR-128 network. *Cell Mol Life Sci*. 2021;79(1):5. doi:10.1007/s00018-021-04068-2
18. Choi HI, Choi J-P, Seo J, et al. Helicobacter pylori-derived extracellular vesicles increased in the gastric juices of gastric adenocarcinoma patients and induced inflammation mainly via specific targeting of gastric epithelial cells. *Exp Mol Med*. 2017;49(5):e330. doi:10.1038/emm.2017.47
19. Yamamoto H, Watanabe Y, Oikawa R, et al. BARHL2 Methylation using gastric wash DNA or gastric juice exosomal DNA is a useful marker for early detection of gastric cancer in an H. pylori-independent manner. *Clin Transl Gastroenterol*. 2016;7(7):e184. doi:10.1038/ctg.2016.40
20. Tanaka F, Takashima S, Nadatani Y, et al. Exosomal hsa-miR-933 in gastric juice as a potential biomarker for functional dyspepsia. *Dig Dis Sci*. 2020;65(12):3493–3501. doi:10.1007/s10620-020-06096-7
21. Martins TS, Vaz M, Henriques AG. A review on comparative studies addressing exosome isolation methods from body fluids. *Anal Bioanal Chem*. 2023;415(7):1239–1263. doi:10.1007/s00216-022-04174-5
22. Dong L, Zieren RC, Horie K, et al. Comprehensive evaluation of methods for small extracellular vesicles separation from human plasma, urine and cell culture medium. *J Extracell Vesicles*. 2020;10(2):e12044. doi:10.1002/jev2.12044
23. Dhondt B, Geeurickx E, Tulkens J, et al. Unravelling the proteomic landscape of extracellular vesicles in prostate cancer by density-based fractionation of urine. *J Extracell Vesicles*. 2020;9(1):1736935. doi:10.1080/20013078.2020.1736935
24. Yang Y, Ji P, Wang X, et al. Bronchoalveolar lavage fluid-derived exosomes: a novel role contributing to lung cancer growth. *Front Oncol*. 2019;9:197. doi:10.3389/fonc.2019.00197
25. Royo F, Théry C, Falcón-Pérez JM, et al. Methods for separation and characterization of extracellular vesicles: results of a worldwide survey performed by the ISEV rigor and standardization subcommittee. *Cells*. 2020;9(9):1955. doi:10.3390/cells9091955
26. Kaddour H, Tranquille M, Okeoma CM. The Past, the Present, and the Future of the Size Exclusion Chromatography in Extracellular Vesicles Separation. *Viruses*. 2021;13(11):2272. doi:10.3390/v13112272
27. Kugeratski FG, Hodge K, Lilla S, et al. Quantitative proteomics identifies the core proteome of exosomes with syntenin-1 as the highest abundant protein and a putative universal biomarker. *Nat Cell Biol*. 2021;23(6):631–641. doi:10.1038/s41556-021-00693-y
28. Abou Zeid F, Charrier H, Beseme O, et al. Lim domain binding 3 (Ldb3) identified as a potential marker of cardiac extracellular vesicles. *Int J Mol Sci*. 2022;23(13):7374. doi:10.3390/ijms23137374
29. Chen Z, Luo L, Ye T, et al. Identification of specific markers for human pluripotent stem cell-derived small extracellular vesicles. *J Extracell Vesicles*. 2024;13(2):e12409. doi:10.1002/jev2.12409
30. Mathivanan S, Fahner CJ, Reid GE, et al. ExoCarta 2012: database of exosomal proteins, RNA and lipids. *Nucleic Acids Res*. 2012;40(Database issue):D1241–4. doi:10.1093/nar/gkr828
31. Keerthikumar S, Chisanga D, Ariyaratne D, et al. ExoCarta: a web-based compendium of exosomal cargo. *J Mol Biol*. 2016;428(4):688–692. doi:10.1016/j.jmb.2015.09.019
32. Pathan M, Fonseka P, Chitti SV, et al. Vesiclepedia 2019: a compendium of RNA, proteins, lipids and metabolites in extracellular vesicles. *Nucleic Acids Res*. 2019;47(D1):D516–D519. doi:10.1093/nar/gky1029
33. Tang Z. GEPIA: a web server for cancer and normal gene expression profiling and interactive analyses. *Pharmacol Ther*. 2017;45(W1):W98–W102.
34. Jahan R, Shah A, Kisling SG, et al. Odyssey of trefoil factors in cancer: diagnostic and therapeutic implications. *Biochim Biophys Acta Rev Cancer*. 2020;1873(2):188362. doi:10.1016/j.bbcan.2020.188362
35. Hoffmann W. TFF2, a MUC6-binding lectin stabilizing the gastric mucus barrier and more (Review). *Int J Oncol*. 2015;47(3):806–816. doi:10.3892/ijo.2015.3090

36. Skryabin GO, Vinokurova SV, Galetsky SA, et al. Isolation and characterization of extracellular vesicles from gastric juice. *Cancers*. 2022;14(14):3314. doi:10.3390/cancers14143314
37. Kagota S, Taniguchi K, Lee S-W, et al. Analysis of extracellular vesicles in gastric juice from gastric cancer patients. *Int J Mol Sci*. 2019;20(4):953. doi:10.3390/ijms20040953
38. Liu WZ, Ma ZJ, Kang XW. Current status and outlook of advances in exosome isolation. *Anal Bioanal Chem*. 2022;414(24):7123–7141. doi:10.1007/s00216-022-04253-7
39. An M, Wu J, Zhu J, et al. Comparison of an optimized ultracentrifugation method versus size-exclusion chromatography for isolation of exosomes from human serum. *J Proteome Res*. 2018;17(10):3599–3605. doi:10.1021/acs.jproteome.8b00479
40. Sidhom K, Obi PO, Saleem A. A review of exosomal isolation methods: is size exclusion chromatography the best option? *Int J Mol Sci*. 2020;21(18):6466. doi:10.3390/ijms21186466
41. Ryu KJ, Lee JY, Park C, et al. Isolation of small extracellular vesicles from human serum using a combination of ultracentrifugation with polymer-based precipitation. *Ann Lab Med*. 2020;40(3):253–258. doi:10.3343/alm.2020.40.3.253
42. Koh YQ, Almughlliq FB, Vaswani K, Peiris HN, Mitchell MD. Exosome enrichment by ultracentrifugation and size exclusion chromatography. *Front Biosci*. 2018;23(5):865–874. doi:10.2741/4621
43. Zhang X, Borg EGF, Liaci AM, et al. A novel three step protocol to isolate extracellular vesicles from plasma or cell culture medium with both high yield and purity. *J Extracell Vesicles*. 2020;9(1):1791450. doi:10.1080/20013078.2020.1791450
44. Webber J, Clayton A. How pure are your vesicles? *J Extracell Vesicles*. 2013;2.
45. Xu X, Cheng J, Luo S, et al. Deoxycholic acid-stimulated macrophage-derived exosomes promote spasmolytic polypeptide-expressing metaplasia in the stomach. *Biochem Biophys Res Commun*. 2020;524(3):649–655. doi:10.1016/j.bbrc.2020.01.159
46. Farrell JJ, Taupin D, Koh TJ, et al. TFF2/SP-deficient mice show decreased gastric proliferation, increased acid secretion, and increased susceptibility to NSAID injury. *J Clin Invest*. 2002;109(2):193–204. doi:10.1172/JCI0212529
47. Nusse R, Clevers H. Wnt/beta-catenin signaling, disease, and emerging therapeutic modalities. *Cell*. 2017;169(6):985–999. doi:10.1016/j.cell.2017.05.016
48. Gao Q, Yang L, Shen A, et al. A WNT7B-m(6)A-TCF7L2 positive feedback loop promotes gastric cancer progression and metastasis. *Signal Transduct Target Ther*. 2021;6(1):43. doi:10.1038/s41392-020-00397-z
49. Vostakolaei MA, Hatami-Baroogh L, Babaei G, et al. Hsp70 in cancer: a double agent in the battle between survival and death. *J Cell Physiol*. 2021;236(5):3420–3444. doi:10.1002/jcp.30132
50. Kahroba H, Hejazi MS, Samadi N. Exosomes: from carcinogenesis and metastasis to diagnosis and treatment of gastric cancer. *Cell Mol Life Sci*. 2019;76(9):1747–1758. doi:10.1007/s00018-019-03035-2
51. Chalmin F, Ladoire S, Mignot G, et al. Membrane-associated Hsp72 from tumor-derived exosomes mediates STAT3-dependent immunosuppressive function of mouse and human myeloid-derived suppressor cells. *J Clin Invest*. 2010;120(2):457–471. doi:10.1172/JCI40483
52. Yuan Q, Yin L, He J, et al. Metabolism of asparagine in the physiological state and cancer. *Cell Commun Signal*. 2024;22(1):163. doi:10.1186/s12964-024-01540-x
53. Chiu M, Taurino G, Bianchi MG, et al. Asparagine synthetase in cancer: beyond acute lymphoblastic leukemia. *Front Oncol*. 2019;9:1480. doi:10.3389/fonc.2019.01480
54. Ye M, Song Y, Pan S, et al. Evolving roles of lysyl oxidase family in tumorigenesis and cancer therapy. *Pharmacol Ther*. 2020;215:107633. doi:10.1016/j.pharmthera.2020.107633
55. Liburkin-Dan T, Toledano S, Neufeld G. Lysyl oxidase family enzymes and their role in tumor progression. *Int J Mol Sci*. 2022;23(11):6249. doi:10.3390/ijms23116249
56. Wang TH, Hsia SM, Shieh TM. Lysyl oxidase and the tumor microenvironment. *Int J Mol Sci*. 2016;18(1):62. doi:10.3390/ijms18010062